Food Biophysics (2012) 7:1–14
DOI 10.1007/s11483-011-9237-9

ORIGINAL ARTICLE

Shear Elastic Deformation and Particle Packing in Plant Cell Dispersions

Patricia Lopez-Sanchez · Vishmai Chapara · Stephan Schumm · Robert Farr

Received: 15 September 2010 / Accepted: 22 September 2011 / Published online: 5 October 2011

Abstract The relationship between small amplitude oscillatory rheological properties and microstructure of plant cell suspensions was studied. Carrot, broccoli and tomato were selected as model plant systems to generate particles with different microstructures: clusters of cells with smooth or rough edges and single cells. By analysing the compressive stress undergone by the plant cells under centrifugation, and comparing this to oscillatory rheometry, agreement was found between the compressive stress required to compress the dispersions to higher insoluble solids dry mass fractions, and the elastic shear modulus of the plant dispersions. This indicated that centrifugation is acting as a crude rheological measurement on the samples, rather than measuring any well-defined "particle phase volume". We estimated the theoretical critical dry mass fraction above which smooth, roughly spherical, elastically interacting particles would acquire a non-zero G′, and compared this with the experimental values. Our results give evidence that for the three vegetable suspensions considered here, the elastic rheology observed is not coming simply from the packing of smooth particles, but is dominated in the dilute limit by attractive forces or interaction of asperities, and in the concentrated limit by deformation and buckling acting together. Improved understanding of the particles and their packing would help in the structuring of food products without adding other texturising or stabilising agents.

Keywords Carrot · Tomato · Broccoli · Dispersion · Rheology · Microstructure · Scanning electron microscopy · Compressive stress

P. Lopez-Sanchez (✉) · V. Chapara · S. Schumm
Structured materials and process science, Unilever R & D,
Olivier Van Noortlaan 120, PO Box 114, 3130 AC, Vlaardingen,
The Netherlands
e-mail: patricia.lopez-sanchez@unilever.com

R. Farr
Unilever R&D,
Colworth Science Park,
Bedford, UK MK441LQ

R. Farr
London Institute for Mathematical Sciences,
22 South Audley Street,
Mayfair, London, UK

Introduction

Dispersions of plant cell particles are interesting systems with the potential to be used as natural structurants in food products reducing the use of gums and stabilisers which are perceived by consumers as artificial. By processing, plant tissues are disrupted, producing a solid and a liquid phase (serum). These dispersions contain insoluble plant particles, such as cell structures and cell fragments, suspended in a liquid phase. While the insoluble plant particles are mainly formed of cellulose, hemicelluloses and pectin, the liquid phase is a solution of sugars and soluble polymers such as pectin (as well as other compounds). The rheological properties of dispersions depend on the rheology of the suspending medium and on the particle volume fraction, which in turn depends on particle attributes such as size, morphology, hardness and particle interactions.[1] Theoretical models have been derived to predict viscosity, yield stress, and modulus of suspensions, both when the particles are dilute, and in the more concentrated regime where they form an elastic network. However the data necessary to apply these theoretical models to plant dispersions are not easy to obtain, due to the deformable and complex nature of plant particles, and they require modifications based on

experimental results.[2, 3] Improved understanding of the particles' packing and the rheological properties would help in the structuring of food products, such as vegetable based soups and sauces, without the addition of other texturising or stabilising agents.

It has been found that the contribution of the liquid phase to the overall rheology of the plant dispersions is very small and no synergistic effect was found between the liquid and the solid phases.[4] The solid particles can be thought of as elastic objects, and this assumption is supported by the fact that some turgor has been reported to be present in the plant cells even when the cell membranes were destroyed by thermal treatment due to the properties of the wall itself.[5] Thus the elastic behaviour of such systems arises mainly from the plant particles. An elastic network of particles may be formed by weak attractive forces, static friction caused by elastic asperities (enabling particles to become entangled, in a similar manner to cogwheels), or the geometric fact that at high concentration even smooth particles must be deformed to fit into the available space. The elastic modulus of such a network is influenced by the elastic properties of the particles. Viscosity can arise from viscous deformation of the liquid phase (long range hydrodynamics or lubrication forces between particles), or direct sliding friction between the particles. The network deformation (and so the viscous dissipation) may be large-scale, or concentrated in discrete, local rearrangement events of particles. The complexity of vegetable suspensions is that all of these factors may operate, and it is not clear which is dominant in a given system and at a given concentration.

The main objective of the present work was to study the linear elastic behaviour of plant cell dispersions. Carrot, broccoli and tomato (major crops in Europe) were selected as plant model systems. The compressive stress undergone by the plant cells under centrifugation was analysed and compared to oscillatory rheometry. The dispersions were produced in order to generate different particle shapes: clusters with smooth or rough edges, and single cells. Measurements were performed over a wide concentration range of insoluble solids corresponding to physical properties varying from liquid-like to paste-like material. We hypothesised about which forces are responsible for the observed behaviour through the whole range of concentrations.

Materials and Methods

Sample Preparation

Fresh carrots (*Daucus carota*, var. Nantes), tomatoes (*S. lycopersicum*, salad variety) and broccolis (*Brassica oleracea*, var. Italica) were purchased from a local supermarket and stored at 5 °C prior to processing. The vegetables were thoroughly washed. Carrots were peeled and cut into approximately 1×1×2 cm pieces. The carrot pieces were mixed with de-ionised water at 1:1 ratio. The sample was placed in a stainless steel vessel for quick heat transfer. The vessel was kept in a hot water bath which was maintained at 90±5 °C, and covered to prevent losses due to evaporation. Thermocouples were attached to three carrot pieces to check that the desired temperature of 90± 5 °C was reached in the core of the pieces, then the vessel was heated, while stirring, for 40 min. After thermal treatment the mechanical disruption was done using a kitchen blender (model 5KSB52, Kitchen Aid, Michigan, USA) at its maximum speed for 3 min. The obtained dispersion was stored at 5 °C until analysis. The tomato dispersion was prepared similarly to carrot with some minor modifications: stem and core were removed and the tomato:water ratio was 9:1 due to the unbound water naturally present in this fruit. The tomato dispersion was sieved through a 1 mm pore size sieve to remove seeds. The large stem and the leaves of broccoli were removed. Based on previous work[4] to obtain clusters with rough edges the broccoli dispersion was prepared by exchanging the order of the thermal and mechanical treatments.

In order to have standardised dispersed particles in sufficient amount the carrot and broccoli suspensions were weighed in several large flasks and centrifuged at 3,500 rpm equivalent to 1,976 g (Centrifuge Beckman Avanthi JA-12, CA, USA). The particle size and morphology of the particles were not significantly affected at this centrifugation speed (images not shown). The supernatants were removed and dilutions were prepared from the sediment. In the tomato initial sample there were enough solids present, therefore the dilutions for tomato were prepared from the initial suspension without centrifugation. Due to the low contribution of the serum phase to the overall rheology, deionised water was used for preparing the dilutions, covering a range from 5 to 90% of sediment (the balance being the added deionised water). Particles were gently mixed with water and the resulting dispersions were left to stabilise overnight (kept at 5 °C).

Measurement of the Particle Size Distribution

The particle size distribution was measured using light scattering (Mastersizer, Malvern Instruments Ltd, Malvern, UK). Approximately 0.5 mL of each sample was pipetted into a water-continuous diluting accessory (2000 Hydro-S) filled with 1,000 mL of deionised water. The particle size distribution was calculated from the intensity profile of the scattered light using the instrument software (Mastersizer 2000, version 5.40). The parameters d(0.1), d(0.5) and d

(0.9) were extracted, which are the sizes such that 10%, 50% and 90% (respectively) of the sample volume consists of particles below this size. The volume-based ($d_{4,3}$) and the area-based ($d_{3,2}$) diameters were also obtained for every sample.

$$d_{(4,3)} = \sum_i n_i d_i^4 / \sum_i n_i d_i^3. \quad (1)$$

$$d_{(3,2)} = \sum_i n_i d_i^3 / \sum_i n_i d_i^2. \quad (2)$$

Where n_i is the number of particles of diameter d_i.

All these parameters are based on the diameter of spherical particles. Throughout this paper, "diameter" will refer to two times the radius of gyration of a particle.

Based on the results obtained by Farr et al,.[6] for a log-normal distribution the width σ can be calculated by $\sigma^2 = \ln\left(d_{4,3}/d_{3,2}\right)$and this can be used to estimate the maximum packing fraction for hard spheres drawn from this distribution.

Light Microscopy

The microstructures generated were observed using light microscopy. Light microscopy images were taken using a Zeiss Axioplan microscope, which was equipped with a video camera (Qicam Qimaging Fast 1394). The samples were diluted 20 times with de-ionised water and slowly stirred. A drop of the prepared sample was placed onto a glass slide and covered with a cover slip. The samples were observed with a 10× dry objective lens along with either differential interference contrast mode (DIC) or bright field. A minimum of six images per sample were taken. The software Linksys 32, version 1.9.6 (Linkam scientific instruments Ltd, UK) was used to control the camera and collect size-calibrated images.

Cryo Scanning Electron Microscopy (Cryo-SEM)

Plant particles in the dispersions (before centrifugation) and in the sediment (after centrifugation) were observed using cryo-SEM. A small aliquot of each sample was placed in a sample holder, frozen in liquid Ethane immediately after processing and stored in liquid Nitrogen. In order to obtain a representative view of the bulk of the sample, the sample was cryo-planed in a cryo-ultramicrotome (Leica Ultracut UCT + EM FCS), first with a glass knife, and the last sections with a diamond knife. For SEM analysis, the sample was briefly sublimated (freeze-etched) at −90 °C in the cryo-preparation chamber (Oxford CT 1500HF) of the microscope (Jeol JSM6340F). After sublimation a layer of Au/Pd of a few nanometres thickness was sputtered onto the surface and the sample was transferred into the microscope. The sample was analysed at −125 °C, at 3 kV and a short working distance of about 6 mm, using the in-lens secondary electron detector (SEI). A collection of approximately 25 images was taken per sample.

Measurement of the Dry Mass Fraction

Dry mass fraction w, was defined as the mass of a dried sample divided by its initial wet mass. Dry mass fraction was determined by drying 5±0.2 g of each sample in a vacuum oven (Memmert GmbH + Co. KG, Schwabach, Germany) at 70 °C and a pressure of 4 KPa for 5 h. The dry mass fraction was calculated, in triplicate, from the sample weight before and after drying.

Measurement of Soluble and Insoluble Solids

The cellulose content in carrot and tomato cell walls is approximately 30% while in broccoli the percentage is lower, around 20%. Pectin content varies between 40 and 60% and it is the major cell wall compound of these three plant materials. Consider therefore each vegetable material, denoted 'veg', in turn. This material will contain insoluble solids, which we assume to be predominantly carbohydrates (or materials of similar dry density) in the form of cellulose and attached hemicelluloses and pectins. This is the cell wall material, and has a dry mass fraction in the vegetable which we denote by w_{ins}^{veg}. The vegetable material will also contain soluble solids, which we assume to be predominantly soluble carbohydrates, at a dry mass fraction w_{sol}^{veg}. The remainder of the vegetable material will be water, which will be present at a mass fraction of $\left(1 - w_{ins}^{veg} - w_{sol}^{veg}\right)$. If the vegetable is processed, it will release serum, which consists of the water containing dissolved soluble solids, and the dry mass fraction of soluble solids in this serum we call

$$w_{serum}^{veg} \equiv w_{sol}^{veg} / (1 - w_{ins}^{veg}). \quad (3a)$$

It is important for all the calculations to follow that we know w_{ins}^{veg} and w_{serum}^{veg}, which allow us to calculate the serum density and volume fraction of dry material in all our samples.

Method 1

The insoluble dry mass fraction w_{ins}^{veg} can be measured for each vegetable material by processing it, then centrifuging and re-suspending the sediment twice in pure water, before measuring the dry mass fraction of the material washed in this way. The quantity w_{sol}^{veg} can be found from this data,

together with total the dry mass fraction of the original processed vegetable.

$$w_{total}^{veg} \equiv w_{ins}^{veg} + w_{sol}^{veg}. \tag{3b}$$

Method 2

As an internal check, we can also calculate w_{ins}^{veg} from the measured values of w_{serum}^{veg} and w_{total}^{veg}, using Eq. 5a,b:

$$w_{ins}^{veg} = \frac{w_{total}^{veg} - w_{serum}^{veg}}{1 - w_{serum}^{veg}}. \tag{3c}$$

These measurements and calculations were performed for the different vegetables on 1:1 dilutions of vegetable:water for carrot and broccoli, and 9:1 for tomato, and the results were then scaled up to values for the pure vegetable.

Centrifugation Experiments, Apparent Volume Fraction and Volume Fraction of Insoluble Solids

Centrifugation experiments were conducted on the batch plant dispersions using different rotational speeds (Centrifuge Beckman Avanthi JA-12, CA, USA). Each experiment was performed in triplicate. The samples were placed in 15 ml calibrated Falcon tubes and the height h_0 (in all cases 6.9 10^{-2} m) and the mass M of the sample were measured. After centrifugation, the height of the sediment column is h, so that there is an apparent volume fraction of solid material in the original sample given by

$$\Psi \equiv \frac{h}{h_0}. \tag{4a}$$

In practice, the surface of the sediment column is rather irregular, so Ψ was measured in a slightly different manner: After centrifugation, the supernatant was carefully removed with a syringe. The ratio Ω between the (wet) mass of the sediment M_{sed} and total amount of centrifuged sample M was calculated:

$$\Omega \equiv \frac{M_{sed}}{M}. \tag{4b}$$

It is therefore necessary to relate the easily measured quantity Ω to the value Ψ which we require, and it is also valuable for the subsequent analysis to know the volume fraction of insoluble solids present in each sample.

If we now consider a sample for centrifugation, which consists of a wet mass fraction $\widehat{w}_{wet}^{veg}$, then this sample will contain a dry mass fraction of soluble and insoluble solids denoted by w_{sol} and w_{ins} which will be given simply by:

$$w_{sol} = \widehat{w}_{wet}^{veg} w_{sol}^{veg} \text{ and } w_{ins} = \widehat{w}_{wet}^{veg} w_{ins}^{veg} \tag{5a, b}$$

We assume that the density of all the dry carbohydrates (soluble and insoluble) are roughly equal, and given by ρ_c= 1500 kg m^{-3} while the density of water is ρ_w= 1000 kg m^{-3}. We also assume that the process of dissolution does not affect the overall volume of a system consisting of water and soluble carbohydrates (an assumption which is correct to within approximately 5% for the case of the soluble carbohydrate sucrose). Under these assumptions, we can calculate the density of the serum phase, (using Eq. 5a,b) as

$$\rho_{serum} = \frac{(1 - w_{ins})}{[(1 - w_{ins} - w_{sol})/\rho_w] + [w_{sol}/\rho_c]}. \tag{6}$$

We define ϕ_0 as the volume fraction of insoluble solids present in the sample, so that the volume fraction of serum (including that permeating the hydrated cell walls) is 1-ϕ_0. This is calculated for each sample from

$$\phi_0 = \frac{w_{ins}/\rho_c}{[w_{ins}/\rho_c] + [(1 - w_{ins})/\rho_{serum}]}. \tag{7}$$

The ratio of the wet mass of the sediment to that of the whole sample will then be given by

$$\Omega = \frac{\rho_c \phi_0 h_0 + \rho_{serum} h - \rho_{serum} \phi_0 h_0}{h_0 [\rho_c \phi_0 + \rho_{serum}(1 - \phi_0)]}. \tag{8}$$

Equations 3a, 3b and 8 can then be rearranged to give an equation which we use to calculate the apparent phase volume Ψ of the sediment in terms of the measured and calculated quantities Ω (ratio of sediment mass to sample mass), ϕ_0 (volume fraction of insoluble material) and ρ_{serum} (the serum density):

$$\Psi = \Omega \left[\frac{\rho_c \phi_0}{\rho_{serum}} + (1 - \phi_0) \right] - \left(\frac{\rho_c - \rho_{serum}}{\rho_{serum}} \right) \phi_0 \tag{9}$$

Rheology Experiments

The rheological measurements were carried out on diluted plant dispersions using a stress controlled rheometer (ARG2, TA Instruments, Delaware, USA) equipped with a 4 blade vane.[7] The vane had a diameter of 12.6 mm and a height of 42.5 mm, and was used in combination with a cup with roughened surfaces and a diameter of 30 mm. All measurements were performed at 20±0.1 °C maintained

with a Peltier system. Approximately 50 mL of sample was loaded into the rheometer. In order to have a controlled history of the samples a pre-shear at 100 s^{-1} for 60 s was applied followed by a resting step of 5 min. The viscoelastic moduli, storage modulus G′ and loss modulus G″, were determined by applying a strain sweep from 0.01 to 300% strain at a frequency of 1 Hz. Values of G′ were selected in the linear region where they are independent of the applied strain.

Results and Analysis

Particle Size and Morphology

Figure 1 shows the morphology of the generated particles. Carrot suspensions contained mainly clusters of cells with smooth edges; cells were separated across the middle lamella, most likely due to pectin solubilisation during the heating step.[8] From the particle size analysis of the suspensions (Figure 2 and Table 1) an average size of the clusters could be estimated. Most of the particles had a diameter between 68 and 319 μm. From the light microscopy images, an average diameter for a carrot cell was estimated as 60 μm, which indicates that the clusters had a diameter of 1 to 5 cells. The broccoli tissues were also disrupted into clusters; however the cells were broken across the cell walls, leading to clusters with rough edges. Furthermore they were larger in size than carrot clusters: most of them containing from 1 up to 11 cells in diameter. The particles in the tomato suspensions were mainly single cells; no clusters were observed under light microscopy. The average diameter of a tomato cell was approximately 250 μm depending on the plane of observation. The particle size measurements indicated also the presence of tomato cell fragments and clusters with a diameter of up to 3 cells, most likely from less abundant tomato tissues, explaining their absence in the light microscopy images.

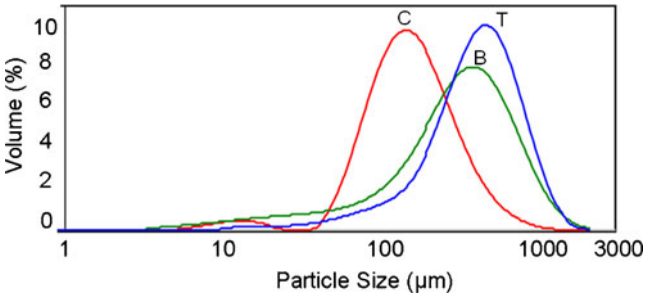

Fig. 2 Typical particle size distributions of C carrot (C), broccoli (B) and tomato (T) dispersions

The volume-based diameter ($d_{4,3}$) gave an average size of approximately 150 μm for carrot, 350 μm for broccoli and 400 μm for tomato. The surface-based diameter ($d_{3,2}$) for carrot and broccoli was 100 μm and for tomato 200 μm. In systems with a broader particle size distribution, like the ones in this study, the volume based particle size parameter $d_{4,3}$ will be highly influenced by large particles whereas the presence of small particles will be reflected in a lower $d_{3,2}$. It is also worth noting that in the systems under study these values, based on light scattering and assuming spherical particles, should be treated with caution, as the particles in the dispersions are certainly not exact spheres.

Amount of Soluble/Insoluble Solids

The results for w_{ins}^{veg} calculated from the serum and the total solids content in Table 2 is lower than when it is measured from a washed sample, which indicates that the washing process was probably incomplete. From this observation (and the generally lower standard deviations of the last two columns in Table 2), we use w_{ins}^{veg} and w_{sol}^{veg} from columns 5 and 6 in Table 2 in all the subsequent calculations.

Particle Packing

Apart from their size and shape, it is important to characterise the packing and deformability of the particles.

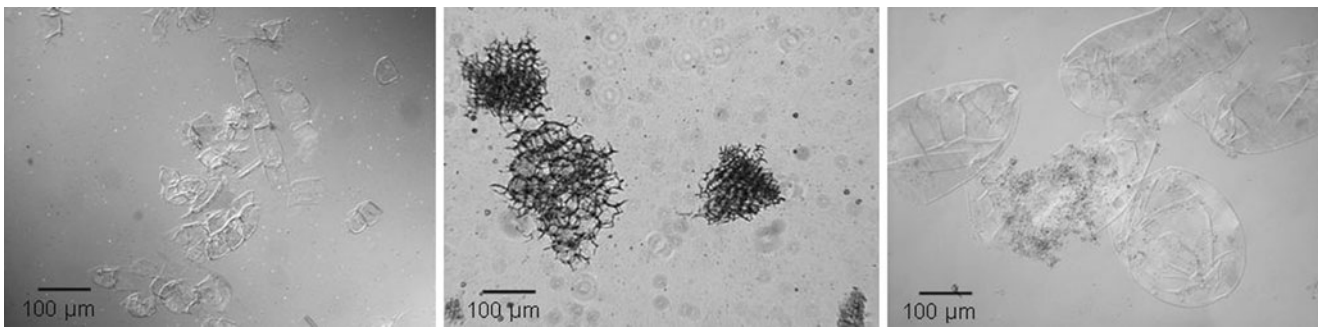

Fig. 1 Light microscopy images showing different particle morphologies. From left to right smooth clusters from carrot, clusters with broken edges from broccoli and individual cells from tomato

Table 1 Particle size distribution of carrot, broccoli and tomato suspensions. The parameters d(0,1), d(0,5) and d(0,9) indicate that 10%, 50% and 90% of the sample volume respectively is occupied by particles below a certain size. $d_{4,3}$ and $d_{3,2}$ are the volume-based and the area-based diameter respectively

Sample	$d_{4,3}$ (μm)	$d_{3,2}$ (μm)	d (0,1) (μm)	d (0,5) (μm)	d (0,9) (μm)
Carrot	158±6	103±1	68±0.2	143±1	319±8
Broccoli	366±17	116±7	68±6	316±12	721±36
Tomato	419±10	233±6	136±4	382±7	752±20

Information about these can be obtained from centrifugation measurements, although the two effects (efficiency of packing and deformability of individual particles) turned out not to be distinguishable by this technique. Figure 3 shows the dependence of the apparent particle volume fraction Ψ on the centrifugation speed. Increasing centrifugation speed produces a steep negative slope, followed by a more gentle decrease of the apparent volume fraction around 3,000–4,000 g. The change in the behaviour was less pronounced for the broccoli samples.

To investigate the effect of centrifugation on the particles, cryo-SEM images were taken before and after centrifugation at 9,000 g. The micrographs (Figure 4) showed that the carrot and tomato particles in the sediment at higher speeds were highly deformed, indicated by buckling of the cell walls (marked with an arrow in the images). In the case of broccoli the cells within the clusters were deformed to particles with a higher aspect ratio. This could indicate that the broccoli clusters were more rigid compared to the other two plant materials. Regardless of these differences, centrifugation is clearly producing significant particle deformation. This deformation will be analysed later in this article in terms of the mechanical properties of the plant material.

Elastic Behaviour of the Plant Cell Dispersions

Small Oscillatory Deformation

In the rheological measurements, dispersions of vegetable matter with different total dry mass fraction w were analysed. For the purposes of plotting, this was converted into volume fraction ϕ_0 of insoluble solids, using Eqs. 5a,b–7 above. For a number of different dilutions, the elastic modulus G′ was measured, under conditions of small deformation and at a frequency of 1 Hz. In all cases the elastic modulus G′ was above the viscous modulus G″ until a certain strain is reached where they cross over and G″ continues above G′.[4] This was the behaviour of all systems over a wide range of concentrations. Dispersions with a volume fraction of insoluble solids below 0.0043 for carrot, 0.0207 for broccoli and 0.0027 for tomato showed particle sedimentation and it was not possible to measure them with the current method.

Estimation of the Compressive Stress Experienced by the Particles During Centrifugation

In addition to the rheological data, suspensions which have an initial volume fraction of insoluble solids ϕ_0 and sample depth h_0 in the centrifuge tube were centrifuged under different accelerations a (measured in terms of the gravitational acceleration g=9.81 m/s^2, and which is assumed to be approximately uniform in the centrifuge tube). This results in a sediment of depth h, with a supernatant above it (Figure 5). Naively, this process can be thought of as measuring the apparent phase volume of the solid matter in the sample, which it was defined as $\Psi \equiv h/h_0$. The terminology of apparent phase volume embodies the idea that centrifugation might overcome the slight attractive forces between the vegetable particles, and compact them down to a well-defined close-packed state, which, in this case, ought to be relatively independent of centrifugation acceleration a. However, this interpretation of Ψ is clearly wrong, since it was found (Figure 3) that Ψ depends strongly on the centrifugation acceleration. Therefore

Table 2 Values of weight fractions of soluble and insoluble material obtained from three replicates of the three different vegetable materials. The last column is the insoluble mass fraction obtained from the total mass fraction and the measured mass fraction of soluble solids in the serum

Sample	w_{total}^{veg} (measured)	w_{ins}^{veg} (measured)	w_{sol}^{veg} from $w_{total}^{veg} - w_{ins}^{veg}$	w_{ins}^{veg} from Eq. 3c	w_{sol}^{veg} from w_{total}^{veg} and Eq. 3c
Carrot	0.093±0.002	0.042±0.014	0.051±0.015	0.032±0.007	0.061±0.011
Broccoli	0.087±0.0002	0.075±0.027	0.011±0.028	0.077±0.011	0.015±0.011
Tomato	0.044±0.0005	0.014±0.0002	0.029±0.0005	0.010±0.002	0.034±0.002

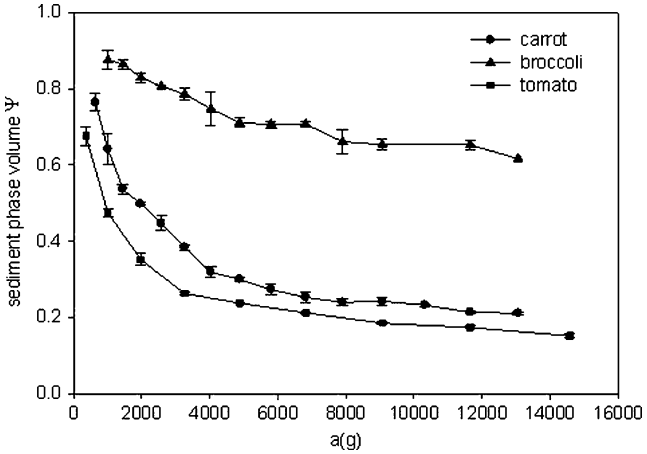

Fig. 3 Apparent sediment phase volume Ψ (height of sediment column divided by height of sample) measured as a function of centrifugation speed a (measured in units of g=9.81 m/s^2) for carrot, broccoli and tomato dispersions. Error bars are based on three replicates

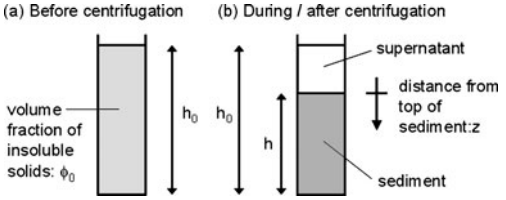

Fig. 5 Schematic representation of the effect of centrifugation on the samples. h_0 represents the height of the sample in the centrifugation tube and h the height of the sediment

this procedure is certainly not measuring a unique and well-defined particle-based phase volume. Instead we propose that centrifugation is acting as another form of rheological measurement. If this interpretation is correct, then the G′ values and centrifugation data should show similar behaviour, or ideally form a single continuous curve when plotted on comparable axes.

From the literature on the rheology of emulsions[9] (which can be seen as model dispersions) it is known that G′ is close in value to the compressive stress Π. As in the study carried out by Mason *et al.*[9] on emulsions, the compressive stress Π was defined to be the pressure exerted on a particle by the packed neighbours around it. It was assumed that this near identity between G′ and Π holds also for these vegetable dispersions. Therefore it is desired to plot both G′ and Π as a function of insoluble solids volume fraction ϕ. The complexity here is that the compressive stress in the sediment during centrifugation is generated by the weight (associated with the effective gravity a, and corrected for buoyancy effects) of the overlying sediment column. The compressive stress Π is therefore a function of height in the column, being zero at the top and maximal at the base.

Two analyses of the centrifugation data were therefore performed: firstly an approximate analysis giving a rough estimate of Π(w) for each centrifugation data point, and secondly a correct but more lengthy analysis, which

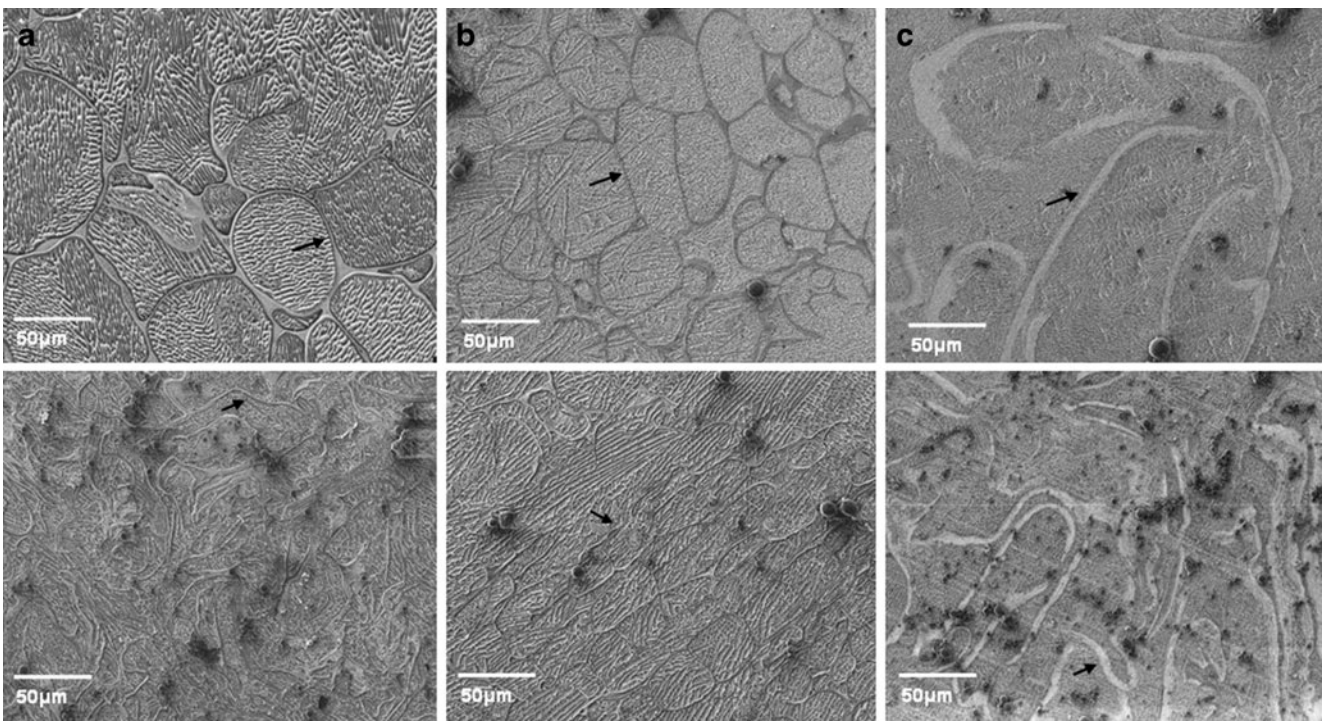

Fig. 4 Particle morphology before (*top*) and after (*bottom*) centrifugation **a**) carrot, **b**) broccoli, **c**) tomato. Cell walls are indicated with an *arrow*

takes into account the depth dependencies in the sediment column itself.

The volume fraction occupied by the insoluble solids in the systems was defined as ϕ, so that the volume fraction occupied by the liquid serum is $(1-\phi)$. For the sediment in a centrifugation experiment, ϕ will be a function of the depth z below the top of the sediment column (Figure 5). The value of ϕ in the uniform sample before centrifugation is denoted ϕ_0, which is calculated for each sample in the manner described in the methods section above.

For a certain point in the sediment column during centrifugation, there are two pressures which should be considered: firstly the hydrostatic pressure in the liquid phase. However, this acts in all directions, both inwards on the outer surface of particles, and outwards on the interior surfaces of hollow particles as well. Thus (neglecting the very slight change in the density of water under pressure), this hydrostatic pressure does not act to compress the sediment. The second pressure is the compressive stress Π, which arises in a similar manner to the hydrostatic pressure, but comes from the (buoyancy adjusted) weight of the overlying sediment particles. It acts between particles, and so can crush them if they are hollow and permeable. Therefore considering the insoluble solids in the sediment column and taking into account the buoyancy, the compressive stress experienced by the particles during centrifugation is governed by the following differential equation:

$$\frac{d\Pi(z)}{dz} = (\rho_c - \rho_{serum})\phi(z)a. \tag{10}$$

Using Eq. 10 it is now possible to solve for Π as a function of ϕ. First, the approximate analysis:

Assume that the solids phase volume everywhere in the sediment is the same, and given by ϕ, so that $\phi=\phi_0 h_0/h$. Therefore from Eq. 10, we see immediately that

$$\Pi(z) = (\rho_c - \rho_{serum})\left(\frac{h_0\phi_0}{h}\right)az. \tag{11}$$

The relevant compressive stress is assumed to be that at the base of the sediment column. Then from each centrifugation experiment and using Eq. 10, a pair of values for the average volume fraction of insoluble solids in the sediment column ϕ and the compressive stress Π at the base of the sediment column can be obtained:

$$(\phi, \Pi) = (\phi_0/\Psi, (\rho_c - \rho_{serum})h_0\phi_0 a). \tag{12}$$

Figure 6 shows the compressive stress (Eq. 11) plotted as a function of the volume fraction ϕ of insoluble solids in the sediment, on the same axes as the G′ from the

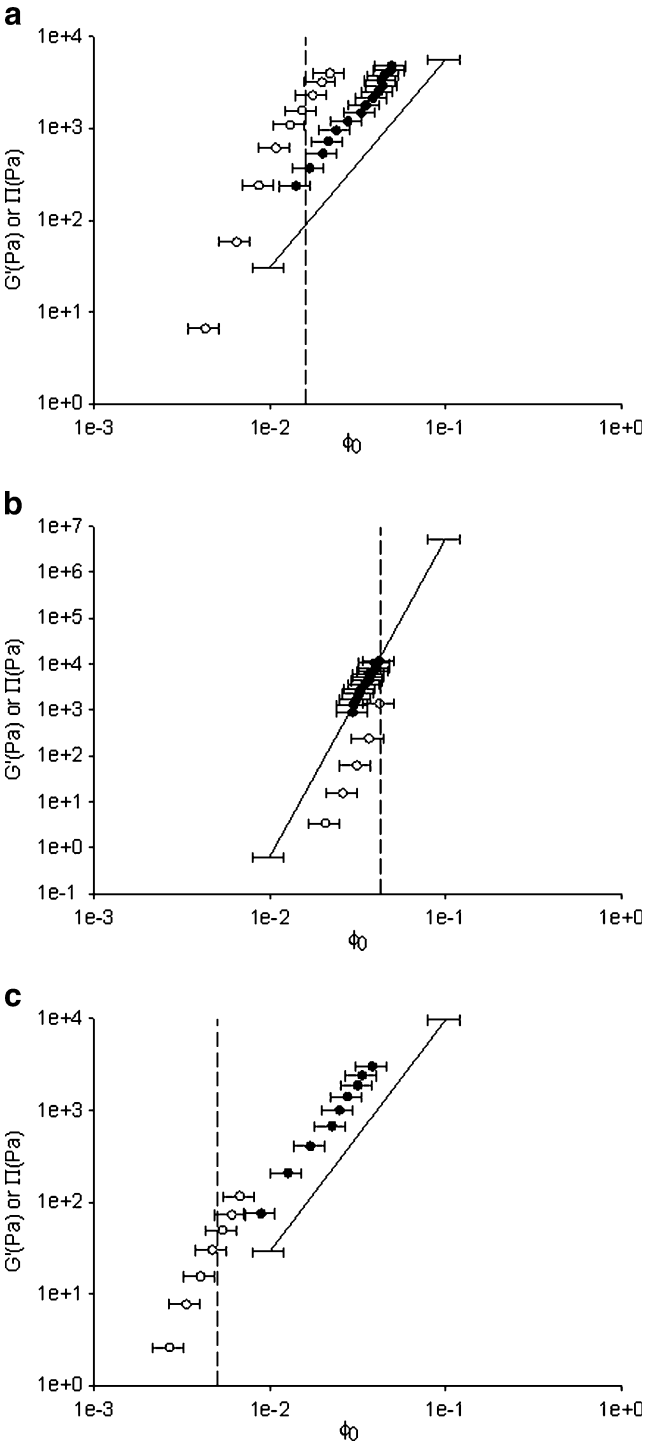

Fig. 6 The plateau value of the elastic modulus G′ (Pa) from rheology measurements (*open symbols*), a first approximation to the compressive stress (*closed symbols*), and the best fit from a more accurate analysis of the osmotic pressure including non uniformity of the centrifuge sediment (*solid line*), as functions of volume fraction of insoluble solids, for **a**) carrot **b**) broccoli and **c**) tomato suspensions. The *dashed line* represents the theoretical critical dry mass fraction for each system at which we predict the system will first become close packed. Very approximate error bars are included based on simple scaling from the uncertainty in w_{ins}^{veg} from Table 1

rheological measurements. As can be observed, the compressive stress Π during centrifugation follows the same slope as G′ (with some offset potentially related to the various approximations above), so does indeed appear to be a crude rheological measurement comparable to G' from shear experiments.

In the crude analysis above, the local volume fraction of solids in the sediment column ϕ(z) was assumed to be the same everywhere. However the sediment column is in fact not uniform. In order to proceed more correctly, a form for the relation between the local values of ϕ and Π was assumed, and the experimental data was used to obtain the parameters in this relationship. The assumption used is that the relationship is a power law:

$$\Pi = \Pi_0 \times [\phi(\Pi)]^n. \tag{13}$$

Where Π_0 and n are constants.

By considering the non-uniformity of the sediment and integrating the exact relationship of Eq. 10 (see Appendix) the following relationship was obtained:

$$a^{-1} = \left\{ \left(\frac{n-1}{n} \right)^n (h_0\phi_0)^{n-1} \frac{(\rho_c - \rho_{serum})}{\Pi_0} \right\} h^n. \tag{14}$$

Equation 14 is a predicted relationship between quantities which were measured in the centrifugation experiments — namely h (obtained from Ψ and Eq. 4a) and a. Therefore those experiments were used to find the best-fitting values of n and Π_0, and the results are shown in Table 3. For broccoli the value of Π_0 obtained was very large compared to carrot and tomato, which indicates that a large compression force is required initially to deform broccoli particles, in agreement with the cryo-SEM images shown above. The extremely large value for $\Pi_0 \sim 10^{13}$ Pa in this case indicates that the power law relationship must break down at higher volume fractions, since close to ϕ=1, the stresses cannot exceed the elastic modulus of pure cellulose, which is in the Giga-Pascal range. Essentially, broccoli appears to have a very high initial stiffness, but at higher volume fractions when the cells are forced to buckle, the increase in G′ with ϕ will become more moderate.

Once the n and Π_0 were obtained, Eq. 13 was used to plot Π versus ϕ_0, where now the only approximation made was the assumed functional form of Eq. 13.

Table 3 Best fit for n and Π_0 constants in Eq. 13

Sample	n	Π_0(Pa)
Carrot	2.26±0.07	$1.0\ 10^{+6}$
Broccoli	6.9±0.4	$4.4\ 10^{+13}$
Tomato	2.52±0.06	$3.2\ 10^{+6}$

The resulting best fitting curves are shown together with the rheological data and the first approximation results in Figure 6. As can be observed, both analyses showed good agreement with the rheological measurements in terms of continuity of the slope, but there is some offset in the absolute values between Π from the centrifugation data and G′ from oscillatory rheology. This offset may be due to remaining approximations in our analysis, or the very close empirical relationship between G′ and Π observed for emulsions not being universally applicable. Nevertheless, we still observe a close relationship between the two measurements, and this is not so unexpected, since the compressive stress is related, like the elasticity, to energy storage in the deformed cell walls.

Estimation of the Critical Dry Mass Fraction for Smooth Particles

If a suspension is composed of individual cells which are smooth spherical elastic particles, there will be a critical concentration at which these cells become close packed. This concentration will be similar to that of the cells in the starting plant tissue, but differ by a small factor due to dilution. Below this concentration, the suspension will not be able to withstand a static shear stress (it will be a liquid), and above it, the particles will be deformed, and a non-zero G′ will result.[10] If there are attractive interactions, or asperities leading to static friction as well, then the system may generate a yield stress at lower concentrations. The theoretical critical dry mass fraction at which the systems would have a G′ due to elastic interactions of smooth, approximately spherical particles was estimated and compared with the experimental values.

For the tomato suspension the microscopy images showed that the particles are mainly single spherical cells. In such a system the volume fraction of insoluble in one spherical cell can be approximated by

$$\phi_{sph} = \frac{4\pi(D/2)^2 t}{(4/3)\pi(D/2)^3} = \frac{6t}{D} \tag{15}$$

where t is the thickness of the cell wall and D the diameter of one cell. Assuming that the critical concentration for a yield stress to appear corresponds to random close packing,[11] then the corresponding critical volume fraction of tomato insoluble solids will be (see Table 4) $\phi^* = 0.76\phi_{sph}$.

Unfortunately, estimating the cell wall thickness from microscopy is inaccurate, due to the available resolution, and possible cell wall swelling effects. Therefore the estimate was based upon the volume fraction of insoluble solids in the undisrupted tomato tissue ($\phi_{intact,T}$) shown in

Table 4 Theoretical predictions for random close packing (RCP) volume fraction of a log-normal distribution of hard spheres[6] with known values of $d_{4,3}$ and $d_{3,2}$

Sample	Width of lognormal distribution σ	Predicted RCP volume fraction
Perfect monodisperse spheres	0	0.64
Carrot	0.65	0.74
Broccoli	1.07	0.81
Tomato	0.77	0.76

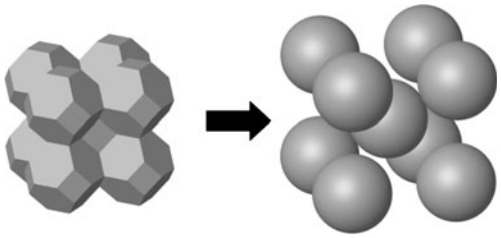

Fig. 7 Schematic picture of the disruption of tomato tissue (modelled as truncated octahedral cells) being disrupted into isolated spherical cells. We assume that the cell wall thickness and surface area of the cells remains unchanged

Table 5, in the following way: assume that in the intact tissue, the cells are truncated octahedra, and that disruption turns these into isolated spherical cells, as shows schematically in Figure 7.

If the surface area of a cell is A, then from simple geometry of a spherical shell, Eq. 15 can be rewritten as

$$\phi_{sph} = A^{-\frac{1}{2}} t \left(3\sqrt{4\pi}\right). \tag{16}$$

Assuming that the surface area and cell wall thickness are the same in a cell when it is part of the intact tissue, then again from elementary geometry, the volume fraction of cellulose in a truncated octahedron can be written as

$$\phi_{intact,T} = A^{-\frac{1}{2}} t \left(\frac{6+12\sqrt{3}}{8\sqrt{2}}\right)^{\frac{3}{2}}. \tag{17}$$

Then the relationship between the phase volume of the cell wall (i.e. insoluble solids) in a sphere and a truncated octahedron is

$$\frac{\phi_{sph}}{\phi_{intact,T}} = 0.973. \tag{18}$$

The final volume fraction of insoluble solids that would be occupied by the tomato particles in the suspension, assuming a random close packing,[11] and considering the starting tomato tissue would then be

$$\phi^* = 0.76\phi_{sph} = 0.74\phi_{intact,T} \tag{19}$$

where $\phi_{intact,T}$ is the volume fraction of insoluble solids in intact tomato tissue. Using Table 5, we obtain $\phi^*=0.0050$ which is shown in Figure 6.

Table 5 Volume fraction of insoluble solids for intact vegetable tissues, calculated using the data in the last two columns of Table 1, and Eqs. 6 and 7

Type of intact tissue	ϕ_{intact}
Carrot	0.022
Broccoli	0.053
Tomato	0.0068

Similarly ϕ^* for carrot and broccoli was obtained. In these two systems the particles are clusters of cells, and therefore the cells in the clusters were assumed to have the same shape as those in the intact plant material, so an estimate for ϕ^* can be found from ϕ_{intact} in Table 5 simply via multiplying by the random close packing fraction in Table 4. The result is $\phi^*=0.016$ for carrot and $\phi^*=0.043$ for broccoli. For comparison these theoretical values are plotted in Figure 6 with the experimental results.

Discussion

Considering a dispersion of plant particles with known geometric properties of size and aspect ratio, then its rheology will have both an elastic and a viscous component. Viscous effects can come from the viscosity of the liquid phase itself (both its flow through the suspension, and lubrication forces between nearly touching particles), as well as friction between particles which touch and slide over one another.

Even more interesting from the viewpoint of texture, are the elastic properties. For the system to display a static elastic modulus, there must firstly be a percolating network of particles, and secondly these particles must not be free to slide past one another under small strains, but instead must be forced to deform in order to accommodate the imposed strain. The interactions between particles can be of various forms, for example steric interactions (particles cannot overlap), electrostatic forces (attractive or repulsive), adhesion from attached (hydrated) polymer chains or van der Waals forces. However, provided all interactions are short-ranged, it is the elastic energy of deformation of the particles which generates the elastic modulus.

Although the elastic modulus derives from the elasticity of the particles, the particle interactions are not inconsequential. They have two essential functions: they determine the geometry of the elastic network (for example, the concentration at which it percolates), and they may also

serve to ensure that the particles do not slide over one another under imposed strain (i.e. ensure that it is, in fact, an elastic network rather than a viscous liquid).

Considering a sequence of dispersions with increasing concentration, then they are expected to pass through a series of regimes of behaviour:

(1) At very low concentration, the particles will not be space-filling: they will sediment under even the weak influence of gravity, or would remain suspended and not touching in the absence of gravity (or a in a density-matched solvent). The system has no elastic modulus or yield stress. This behaviour was observed for the dispersions with a volume fraction of insoluble solids below 0.0043 for carrot, 0.0207 for broccoli and 0.0027 for tomato.

(2) At some concentration, a percolated network will form. If the system at this stage is dominated by attractive forces, then this may happen at a very low concentration: attractive particles are able to flocculate, forming fractal clusters,[12] which aggregate into a weak gel, at very low number densities. Such a system will yield and flow only when these attractive bonds break. On the other hand, the particles may just have short range repulsive interactions. If there are asperities on the surface, this may mean that the particles withstand static friction, so that they can roll over each other, but not easily slide (like cogwheels in two dimensions). In this case, a percolated structure at a higher packing fraction than for flocculated particles is expected, but a lower packing fraction than for smooth repulsive objects. This fraction will be related to random loose packing,[13] which for spheres occurs at a volume fraction a little higher than 50%, but is less for non-spherical particles. In the random loose packed state, the surface roughness/asperities of the particles must be deformed in order to allow particles to exchange places, and thus for the system to yield. Lastly, if the particles are smooth, then they will form a percolated network only at random close packing, which for spheres[11] is 64% and for non-spherical particles may be lower.[14] Polydispersity will also affect these packing fractions.[6] In the random close packed state, it is purely steric interactions that count: a particle must change its overall shape in order to move past its neighbours. For our systems, the random close packed state was calculated to occur for insoluble solids volume fractions ϕ_0 above 0.016, 0.043 and 0.0050 for carrot, broccoli and tomato respectively. These are considerably higher than the observed volume fractions at which sedimentation occurs. This strongly indicates that at low volume fraction, all systems are dominated by interactions other than steric repulsion of smooth, elastic bodies: either asperities or weak attractive interactions are lowering the critical packing fraction.

(3) As the concentration is increased above the percolation threshold, the elastic modulus will increase, and the particles are likely to be increasingly deformed, even when there is no imposed strain. It is also possible that the dominant interaction supporting the network may change. For example, an open, low density network supported by attractive forces may collapse under the pressure of added particles. The system may then re-arrange at a higher density where it is supported by frictional effects (like a pile of cogwheels) or purely steric/packing effects (like a collection of smooth spheres).

(4) Finally, at very high concentrations, the particles will necessarily be highly deformed, in order to fit into the available space. This can be seen in the cryo-SEM images, where buckled cell walls and crushed cells are clearly evident. In this regime, steric effects alone will be enough to prevent liquid-like flow of the system (although friction and attractive forces may also be present). More particularly, the elastic modulus should be determined purely by the deformation of the particles, and thus depend upon how far the concentration exceeds random close packing.

An important question to ask is what interactions are producing the elastic properties in these systems. If the relevant interactions are purely shape/packing effects of smooth, repulsive particles, then the control of the rheological properties of the plant dispersions could be performed by affecting the aspect ratio and size distribution of the particles. On the other hand, if it is frictional interactions from asperities which dominate, then the surface roughness of particles will be critical, and the elastic properties (especially at low concentration) could be modified by, for example, choosing hot-break or cold-break processing.[4] Lastly, if attractive forces dominate, then (again at low concentration), the elastic properties should be sensitive to solvent quality, or the presence of cations such as Ca^{2+}, which can affect the interactions of soluble polysaccharides attached to the cell wall surfaces.

For the three vegetable suspensions considered here, G′ arises at lower concentrations than the theoretical critical concentration based on packing of smooth elastic particles. This indicates that something other than pure elastic interactions of smooth objects are acting in the systems to generate an elastic network. It is suggested that at low mass fractions, the elastic network is stabilized by weak attractive interactions between the particles, aided (for the rough

clusters) by entanglements of asperities. As concentration increases, there is no jump in the stress versus mass fraction curves, which maintains a simple power-law behaviour (up to the highest centrifugation stresses studied here). Therefore it appears that there is a smooth crossover from a network generated by attractive and frictional interactions to one formed by steric interactions of deformed particles, and a gradually increasing deformation of the particles should be present over the whole range of concentrations w, culminating with the highly deformed particles seen in the cryo-SEM images.

The centrifugation experiments also indicated that there is no clear gap between the overcoming of adhesive or frictional forces and deformation of the particles. Both processes occur simultaneously: particles settled and started to be deformed under a certain compressive stress and above this stress the deformation of the particles continued, clearly reflected as buckling of the cell walls in the cryo-SEM images. Furthermore the compression under centrifugation was irreversible, so that bulking of cell walls (coupled perhaps to adhesive interactions) is likely irreversible.

Based on the differences between the theoretical and the experimental critical concentrations (onset of G′), the contribution of attractive plus frictional forces seems to increase in the order tomato < carrot < broccoli. The forces due to roughness or adhesiveness of the particles should be higher for broccoli, where cell wall debris is attached to the cell clusters, and they should be lower for the tomato suspension, which is mainly formed of (visually) smooth single cells (Figure 1). Furthermore for broccoli, the forces required to deform the particles are higher than for carrot and tomato, indicated by a steep function (Figure 6b). This might reflect differences in the stiffness of the cell walls, or that the rough surface of the broccoli clusters, compared to carrot and tomato cells, would require a higher force to pack the particles to lower phase volumes.

Lastly, other attractive forces such as electrostatic interactions from polymers on the surfaces might also be present. The action of endogenous enzymes such as PME on the pectin of cell walls of broccoli could increase the charge on the surface of the particles, raising the possibility of significant electrostatic interactions. The charge in carrot and tomato particles will not be increased by the action of endogenous enzymes however, as the thermal process applied prior to mechanical disruption would inactivate the enzymes; thus electrostatic interactions are less likely. Our own rheological experiments (data not shown), in the presence of 0.5–2% KCl and $CaCl_2$ did not show a significant effect on the viscoelastic properties of carrot suspension, indicating that the above made assumption is valid.

Conclusions

By analysing the compressive stress undergone by the plant cells under centrifugation, and comparing this to oscillatory rheometry, quantitative agreement in terms of slope and approximate agreement in terms of absolute values was found between the compressive stress required to compress the dispersions to higher insoluble solids dry mass fractions, and the shear elastic deformation of the plant dispersions. This indicated that centrifugation is acting as a crude rheological measurement on the samples, rather than measuring any well-defined "particle phase volume". Our results give evidence that for the three vegetable suspensions considered here, the elastic rheology observed is not coming simply from the packing of smooth particles, but is dominated in the dilute limit by attractive forces or interaction of asperities, and in the concentrated limit by deformation and buckling acting together. The viscous component to the rheology may arise from direct sliding friction between particles, hydrodynamic lubrication forces and the viscosity of the liquid phase (long range hydrodynamics), and our results are not able to distinguish between these.

Acknowledgments The authors would like to thank Maud Langton for proof reading of manuscript draft. This work was financially supported by the Commission of the European Communities, Framework 6, Priority 5 'Food Quality and Safety', STREP Project Healthy Structuring 2006–023115.

Appendix

In the approximate analysis in the body of the text, the volume fraction of insoluble solids in the sediment, $\phi(z)$, was assumed to be independent of z. However, in reality, the sediment column will not be uniform, since particles further from the surface will be compressed by a greater weight of overlying particles. To proceed, we make the assumption that there is a power law relationship between the local osmotic pressure and the local volume fraction of insoluble solids, *viz*:.

$$\Pi = \Pi_0 \times [\phi(\Pi)]^n \tag{A.1}$$

Where Π_0 and n are constants, and the validity of this power law can be checked *a posteriori*.

Then from Eq. 10 in the text,

$$\frac{d\Pi}{dz} = (\rho_c - \rho_{serum})\phi(z)a = (\rho_c - \rho_{serum})\left(\frac{\Pi}{\Pi_0}\right)^{1/n} a$$

so

$$\int \frac{1}{\Pi^{1/n}} \frac{d\Pi}{dz} dz = \frac{(\rho_c - \rho_{serum})a}{{\Pi_0}^{1/n}} z + C$$

where C is an integration constant, which vanishes because the osmotic pressure at the top of the sediment column is zero. Thus

$$\frac{\Pi^{1-1/n}}{1-1/n} = \frac{(\rho_c - \rho_{serum})a}{{\Pi_0}^{1/n}} z \tag{A.2}$$

Now, the volume of insoluble solids before centrifugation is

$$V = Ah_0\phi_0$$

where A is the cross sectional area of the column, and after centrifugation

$$V = A\int_0^h \phi(z)dz$$

Therefore

$$\int_0^h \phi(z)dz = h_0\phi_0 \tag{A.3}$$

From Eqs. A.1 and A.2 ϕ in terms of z will be:

$$\phi = \left(\frac{\Pi}{\Pi_0}\right)^{1/n} \equiv \left(\left(\frac{\Pi}{\Pi_0}\right)^{1-1/n}\right)^{\frac{1}{n-1}}$$

$$= \left[\left(\frac{(1-1/n)(\rho_c - \rho_{serum})az}{\Pi_0}\right)\right]^{\frac{1}{n-1}} \tag{A.4}$$

Using Eqs. A.3 and A.4

$$h_0\phi_0 = \int_0^h \phi(z)dz = \left(\frac{n-1}{n}\right)\left[\frac{(1-1/n)(\rho_c - \rho_{serum})a}{\Pi_0}\right]^{\frac{1}{n-1}} h^{\frac{n}{n-1}}$$

And so, simplifying slightly, we obtain:

$$h_0\phi_0 = \left(\frac{n-1}{n}\right)^{\frac{n}{1-n}}\left[\frac{(\rho_c - \rho_{serum})a}{\Pi_0}\right]^{\frac{1}{n-1}} h^{\frac{n}{n-1}}$$

which can be re-arranged to give

$$a^{-1} = \left\{\left(\frac{n-1}{n}\right)^n (h_0\phi_0)^{1-n}\frac{(\rho_c - \rho_{serum})}{\Pi_0}\right\} h^n \tag{A.5}$$

What is known experimentally, is $\Psi \equiv \frac{h}{h_0}$ in terms of ϕ_0, and we also know the values of h_0, as well as ρ_c and ρ_{serum} [the latter from Eq. 6 in the text].

We can thus plot h against ϕ_0 from the centrifugation data, and fit this to Eq. A.5 to obtain the best fitting values for n and Π_0. Once we have those values, Eq. A.1 is used to plot Π vs ϕ_0.

Symbols

Π	osmotic pressure from compressive stress (Pa)
ρ_c	density of dry carbohydrates (kg m^{-3})
ρ_w	density of water (kg m^{-3})
ρ_{serum}	density of serum phase in each sample (kg m^{-3})
ϕ_0	volume fraction of insoluble solids in sample before centrifugation (no units)
ϕ	volume fraction of insoluble solids in a local region of a sample (no units)
ϕ_{sed}	volume fraction of insoluble solids in the sediment (no units)
ϕ^*	critical volume fraction of insoluble solids at particle close packing (no units)
Ψ	apparent volume fraction (ratio of sediment height to sample height) (no units)
Ω	mass ratio M_{sed}/M (no units)
A	surface area of one cell (m^2)
D	diameter of one cell (m)
h_0	height of centrifugation sample (m)
h	height of sediment after centrifugation (m)
M	mass of centrifugation sample (kg)
M_{sed}	wet mass sediment after centrifugation (kg)
t	thickness of the cell wall (m)
w	dry mass fraction of sample (no units)
w_{total}^{veg}	dry mass fraction of all solids in vegetable of type 'veg' (no units)
w_{ins}^{veg}	dry mass fraction of insoluble solids in vegetable of type 'veg' (no units)
w_{sol}^{veg}	dry mass fraction of soluble solids in vegetable of type 'veg' (no units)
w_{serum}^{veg}	dry mass fraction of soluble solids in the serum from vegetable type 'veg' (no units)
$\hat{w}_{wet}^{veg}$	wet mass fraction of vegetable type 'veg' in the centrifugation sample (no units)
w_{ins}	dry mass fraction of insoluble solids in sample (no units)
w_{sol}	dry mass fraction of soluble solids (assumed carbohydrates) in sample (no units)

References

1. C.W. Macosko, *Rheology: Principles, Measurements and Applications* (VCH publishers, New York, 1994), pp. 425–474
2. D.B. Genovese, J.E. Lozano, M.A. Rao, The rheology of colloidal and non-colloidal food dispersions. J. Food Sci. **72**, R11–R20 (2007)
3. L. Day, M. Xu, S.K. Øiseth, L. Lundin, Y. Hemar, Dynamic rheological properties of plant cell-wall particle dispersions. Colloids Surf. B Biointerfaces **81**, 461–467 (2010)

4. P. Lopez-Sanchez, J. Nijjsse, H.C.G. Blonk, L. Bialek, S. Schumm, M. Langton, Effect of mechanical and thermal treatments on the microstructure and the rheological properties of carrot, broccoli and tomato dispersions. J. Sci. Food Agric. **91**, 207–217 (2011)
5. I. Shomer, P. Lindner, R. Vasiliver, Mechanism which enables the cell wall to retain homogeneous appearance of tomato juice. J. Food Sci. **49**, 628–633 (1984)
6. R.S. Farr, R.D. Groot, Close packing density of polidisperse hard spheres. J. Chem. Phys. **131**, 244104 (2009)
7. Q.D. Nguyen, D.V. Boger, Yield stress measurement for concentrated suspensions. J. Rheol. **27**, 321–349 (1983)
8. L.C. Greve, R.N. McArdle, J.R. Gohlke, J.M. Labavitch, Impact of heating on carrot firmness: changes in cell wall components. J. Agric. Food Chem. **42**, 2900–2906 (1994)
9. T.G. Mason, J. Bibette, D.A. Weitz, Elasticity of compressed emulsions. Phys. Rev. Lett. **75**, 2051–2054 (1995)
10. T.G. Mason, J. Bibette, D.A. Weitz, Yielding and flow of monodispersed emulsions. J. Colloid Interface Sci. **179**, 439–448 (1996)
11. J.D. Bernal, J. Mason, Packing of spheres: co-ordination of randomly packed spheres. Nature **188**, 910–911 (1960)
12. D.A. Weitz, M. Oliveria, Fractal structures formed by kinetic aggregation of aqueous gold colloids. Phys. Rev. Lett. **52**, 1433–1436 (1984)
13. C. Song, P. Wang, H.A. Makse, A phase diagram for jammed matter. Nature **453**, 629–632 (2008)
14. G.W. Delaney, P.W. Cleary, The packing properties of superellipsoids. Europhys. Lett. **89**, 34002 (2010)